

Attenuation of hepatic ischemia-reperfusion injury by adipose stem cell-derived exosome treatment via ERK1/2 and GSK-3 β signaling pathways

YAQING ZHANG^{1*}, YONGHUA LI^{1*}, QILONG WANG^{1*}, DONGYU ZHENG¹, XUE FENG², WEI ZHAO³, LINLIN CAI⁴, QINGQING ZHANG⁵, HAITAO XU¹ and HAILONG FU¹

¹Department of Anesthesiology, Changzheng Hospital, Naval Medical University, Shanghai 200003; ²Department of Liver Surgery and Liver Transplantation Center, Renji Hospital, School of Medicine, Shanghai Jiao Tong University, Shanghai 200127; ³Department of Obstetrics and Gynecology, Inner Mongolia Autonomous Region Corps Hospital of Chinese People's Armed Police Force, Hohhot, Inner Mongolia Autonomous Region 010040; ⁴Department of Anesthesiology, Wuxi People's Hospital, Wuxi, Jiangsu 214023; ⁵Department of Anesthesiology, Shanghai Pulmonary Hospital, School of Medicine, Tongji University, Shanghai 200433, P.R. China

Received March 17, 2021; Accepted October 14, 2021

DOI: 10.3892/ijmm.2021.5068

Abstract. Exosomes are an emerging therapeutic tool for the treatment of tissue injuries. In the present study, the protective effect of isolated exosomes from adipose-derived stem cells (ADSCs-exo) against hepatic ischemia-reperfusion (I/R) injury was explored. Hepatic I/R injury was achieved by inducing ischemia for 60 min followed by reperfusion for 2 and 6 h. Pre-treatment with ADSCs-exo revealed a significant reduction in necrosis and apoptosis in liver tissue induced by I/R injury. Hypoxic oxidative stress was managed by exosome-mediated reduced reactive oxygen species and increased superoxide dismutase that in turn protected mitochondrial damage and apoptosis. Reduction in inflammatory mediators such as IL-1 β and TNF- α was also observed and protection of hepatocytes from I/R injury was evidenced by a significant decrease in biochemical markers of liver damage (alanine transaminase, aspartate transaminase and lactate dehydrogenase). Exosomal prostaglandin E2 (PGE2)-mediated ERK1/2 and GSK-3 β phosphorylation were revealed to increase Bcl-2 and decrease Bax expression with mitochondrial permeability transition pore-inhibition which may be considered a prime mechanism

of exosome-mediated hepatoprotection. In conclusion, our results indicated that ADSCs-exo pre-treatment is effective in protecting liver I/R injury.

Introduction

Hepatic ischemia-reperfusion (I/R) injury is a common cause of postoperative complications or liver damage, and is also considered a major reason for post-transplantation liver-graft dysfunction (1,2). During I/R injury, oxidative phosphorylation is inhibited by hypoxia that results in anaerobic glycolysis (3). The generation of reactive oxygen species (ROS), lipid peroxidation and dsDNA damage are prime mechanisms consequently associated to I/R injury (4,5). ROS generated by mitochondria and release of inflammatory mediators from the endoplasmic reticulum result in upregulation of autophagy-related genes (6,7). Several attempts have been made to control hepatic I/R injury. For instance, Chen *et al* reported that dexmedetomidine could protect the liver from I/R injury by decreasing inflammatory response associated with NLRC5 (8). In addition, oleanolic acid (9), l-tetrahydropalmatine (10), hyperoside (11), cerium oxide nanoparticles (12) have also been reported to have a protective role against hepatic I/R injury.

Regenerative medicine based on stem cell therapy is a new area in medicine that offers treatment of degenerative disorders and injuries. However, implanted stem cells face certain challenges such as poor survival particularly in hypoxic conditions causing poor therapeutic response (13,14). Saidi *et al* used human adipose-derived mesenchymal stem cells (hADMSCs) against hepatic I/R injury in a mouse model (15). They identified that infusion of 1-2 million hADMSCs 30 min prior to ischemia could decrease I/R injury (15). In another study, Saat *et al* determined that C57BL/6 mice-derived MSCs were ineffective against hepatic I/R injury (with hepatectomy) when

Correspondence to: Dr Hailong Fu or Dr Haitao Xu, Department of Anesthesiology, Changzheng Hospital, Naval Medical University, 415 Fengyang Road, Shanghai 200003, P.R. China
E-mail: fuhailong1979@163.com
E-mail: xuht1968@163.com

*Contributed equally

Key words: adipose-derived stem cells, exosomes, hepatic ischemia-reperfusion injury, oxidative stress, ERK/GSK-3 β

cells were infused 2 h prior or 1 h following ischemia (16). It was observed that within 2 h, infused cells disappeared, and the remaining cells could not reach the area of the injury (16). Additionally, the necessity of phenotypically stable cells, higher cost, handling complications, risk of rejection following implantation and potential risk of ectopic tissue/tumor formation are other challenges in the application of stem cells. To avoid such drawbacks related to the administration of stem cells, exosomes have emerged as a new tool to achieve therapeutic outcomes with prolonged circulatory life. Exosomes are bi-layered vesicles that are released by cells for intercellular signaling (17). They contain proteins, lipids and nucleic acids (18). Among them, microRNAs (miRNAs or miRs) were reported to induce the therapeutic effect of exosomes (18). Exosomes derived from stem cells have exhibited various therapeutic responses such as promotion of wound healing (13), recovery of neurological function following nerve injury (18), and protection against kidney injury (19) and erectile dysfunction (20). Recently, their potential for the treatment of severe COVID-19 was also proposed (21).

Adipose-derived stem cells (ADSCs) were found to attenuate hepatic I/R injury in swine models by decreasing oxidative stress (22). Based on research concerning the therapeutic potential of exosomes which is similar to stem cells, it was hypothesized that exosomes derived from ADSCs (ADSCs-exo) may protect hepatic I/R injury and these exosomes have greater potential for clinical translation considering drawbacks related to direct stem cell therapy. The present study aimed to investigate the protective efficacy of ADSCs-exo against hepatic I/R injury. ADSCs-exo were isolated from ADSC culture medium through the differential centrifugation process. These exosomes were evaluated for their efficacy through pre-treatment via the portal vein of an animal model.

Materials and methods

Animals. Male Sprague-Dawley rats (n=41; 6 weeks old), weighing 160-200 g, were purchased from Sino-British SIPPR/BK Lab Animal Ltd. (Shanghai, China). The animals were housed in a pathogen-free environment with standard conditions of temperature (27±2°C), humidity (50±5% RH) and a 12-h light/dark cycle. All of the animals were provided with 24-h free access to food and water. All procedures were conducted in accordance with the Guide for the Care and Use of Laboratory Animals of the National Institutes of Health and was approved (approval no. 00100097) by the Medical Ethics Committee of Naval Medical University (Shanghai, China).

Isolation of ADSCs-exo. ADSCs were isolated from the inguinal fat. Briefly, 5 rats were euthanized by intraperitoneal injection of sodium pentobarbital (100 mg/kg). Following confirmation of death by lack of pulse, breathing and corneal reflex, the abdomen and back of rats were disinfected using 75% alcohol and placed under an aseptic environment. The skin from both sides of the abdomen in the groin region was removed using scissors to expose fat pads. Fat pads were clamped using an Allis tissue clamp and removed using ophthalmic scissors. A total of 4-5 ml of fat tissue from each rat was obtained under sterilized conditions, and was digested

with collagenase type I (0.25%) for 50 min at 37°C with shaking using a laboratory shaker. Following digestion, high sugar DMEM containing 10% FBS (both from Life Technologies; Thermo Fisher Scientific, Inc.) and standard concentrations of penicillin (10 U/ml) and streptomycin (100 µg/ml; both from Shanghai Yeasen Biotechnology Co., Ltd.) was added to the fat mixture followed by filtration through a cell strainer. Subsequently, following appropriate dilution, the supernatant was centrifuged at 1,000 x g for 10 min at 25°C to collect cells that were further cultured in 10 cm² cell culture plates. Following the third passage of cells, surface markers CD73, CD90, CD105, CD34, CD45 and CD11b were identified using marker identification kit Oricell[®]; cat. no. RAXMX-09011; [Saiye (Guangzhou) Biotechnology Co., Ltd.] according to the manufacturer's protocol, and a flow cytometer (BD LSR II; BD Biosciences).

The third generation of ADSCs was cultured at 37°C and 5% CO₂ in a petri dish with complete medium, and after 80% confluency was reached, the medium was replaced with serum-free medium that was collected after 48 h. The collected serum-free medium was centrifuged at 400 x g for 15 min at 4°C to remove floating cells. The supernatant was collected and centrifuged at 10,000 x g for 15 min at 4°C to remove cellular debris. Exosomes were collected through ultracentrifugation at 100,000 x g for 13 h at 4°C. Subsequently, the exosomes were gently washed with PBS and collected through centrifugation at 14,000 x g for 10 min at 4°C. Collected exosomes were observed under transmission electron microscopy (TEM) and surface markers including TSG101 (1:1,000; product code ab83), CD9 (1:1,000; product code ab92726) and CD63 (1:1,000; product code ab193349; all from Abcam) were identified using western blot analysis according to the manufacturer's protocol.

Surgical procedures. A total of 36 SD rats were divided into three groups: Sham-operated rats (Sham), PBS-treated rats for I/R injury (PBS + I/R) and exosome-treated rats for I/R injury (ADSCs-exo + I/R). Rats were fasted 12 h prior to the experiment. For the surgical procedure, rats were anesthetized by intraperitoneal (i.p.) injection of 1% pentobarbital sodium (45 mg/kg of body weight). Following midline laparotomy, the portal vein and portal artery were clamped to induce 70% hepatic ischemia. A total of 50 µl exosomes (30 µg) were administered via the portal vein before induction of ischemia in rats included in the ADSCs-exo + I/R group while a similar volume of PBS was administered in rats in the PBS + I/R group (Fig. 1). Ischemia was maintained for 60 min followed by reperfusion. During experimental procedures, the rats were placed on a 37°C warmed surface. Following 2 and 6 h of reperfusion, rats (n=6, for each time-point) were sacrificed using 100 mg/kg intraperitoneal injection of pentobarbital sodium and liver and serum samples were collected for further examination. The death of the rats was confirmed by lack of pulse, breathing and corneal reflex. For the sham group, the same procedure was followed without clamping of hepatic vessels.

Biochemical analysis. Collected blood was centrifuged at 1,000 x g for 15 min at 4°C to obtain serum that was analyzed for quantification of alanine aminotransferase (ALT), aspartate

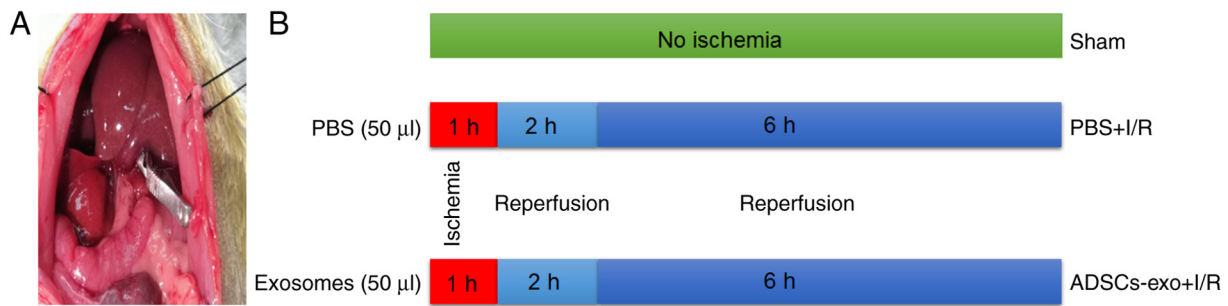


Figure 1. (A) Image demonstrating midline laparotomy and clamping of the portal vein and artery. (B) Grouping of animals and illustration of the experimental protocol. I/R, ischemia-reperfusion; ADSCs-exo, exosomes from adipose-derived stem cells.

aminotransferase (AST) and lactate dehydrogenase (LDH) using commercial kits (cat. no. ALT000A, AST000S and LDH000S for ALT, AST and LDH, respectively; from Beijing Autobio Co. Ltd.) following the manufacturer's protocol on Auto-Analyzer (TBA-120FR; TOSHIBA).

Antioxidant enzymes and lipid peroxidation analysis. The levels of malondialdehyde (MDA; cat. no. MBS727531; MyBioSource, Inc.), superoxide dismutase (SOD; cat. no. MBS266897; MyBioSource, Inc.) and ROS (cat. no. LS-F9759; LifeSpan BioSciences, Inc.) were determined in liver homogenates using a commercial testing kits according to the manufacturer's protocol.

Determination of inflammatory markers. The expression levels of interleukin (IL)-1 β (product code ab255730; Abcam) and TNF- α (product code ab236712; Abcam) were detected in rat serum using respective ELISA kits.

cAMP and PGE2 assay levels. The amount of cAMP in serum was quantified using cAMP Complete ELISA kit (product code ab133051; Abcam). Furthermore, prostaglandin E2 (PGE2) was also quantified in serum using PGE2 ELISA kit (product code ab133021; Abcam).

Histological analysis. Following 2 and 6 h of reperfusion, collected liver tissue samples were fixed in 4% formaldehyde solution for 12 h at 4°C. The tissue was dehydrated and embedded in paraffin (23). Embedded tissues were sliced into 5- μ m thick sections. For necrosis evaluation, hematoxylin and eosin (H&E) staining was performed according to the manufacturer's protocol (Beyotime Institute of Biotechnology). Briefly, hematoxylin staining solution was added on specimens for 5 min at room temperature followed by washing with tap water for 1-2 min. The slides were dipped in 1% hydrochloric acid in 70% ethanol for 10 sec followed by washing with tap water for 10 min. Eosin staining solution was added on specimens for 30 sec and directly immersed in 95% ethanol followed by absolute ethanol for 10 sec. Necrotic areas were quantified using ImageJ software (version 1.51j8; National Institutes of Health). TdT-mediated dUTP nick-end labeling (TUNEL) staining was also performed to observe apoptotic cells in liver samples using a commercial kit (cat. no. 11684817910; Roche Diagnostics), following the manufacturer's protocol. Briefly, TUNEL reaction mixture (50 μ l) was

added onto specimens and placed at 37°C for 1 h in a dark humidified box. After washing with PBS (three times for 3 min each), 50 μ l converter-peroxidase was added to specimens for 30 min at 37°C for 1 h in a dark humidified box followed by DAB staining for 30 min at 25°C. Stained samples were observed using light microscope (Olympus CX41; Olympus Corporation). The percentage apoptotic cells was counted using the following formula: (Number of apoptotic cells/total number of cells) x100.

For immunohistochemical analysis, liver samples were fixed using 4% paraformaldehyde (in normal saline) for 10 min at room temperature, and further sliced into 30- μ m-thick sections. Following washing with PBS, permeabilization was performed using washing buffer with 0.3% H₂O₂ and 0.5% Triton X-100. Sections were incubated with respective primary antibodies including ERK1/2 (1:1,000; product no. 4695), p-ERK1/2 (1:2,000; product no. 4370), GSK-3 β (1:1,000; product no. 5676) and p-GSK-3 β (1:1,000; product no. 9322; all from Cell Signaling Technology, Inc.) at 4°C overnight after blocking non-specific binding sites with 3% BSA (Shanghai Yeasen Biotechnology Co., Ltd.) for 1 h at room temperature. Samples were washed and incubated in secondary antibodies (HRP-goat anti-mouse IgG, cat. no. GB23301 for ERK1/2 and GSK3 β and HRP-goat anti-rabbit IgG, cat. no. GB23303 for p-ERK1/2 and p-GSK3 β ; both from Servicebio) at 1:200 dilution for 1 h at room temperature followed by staining with DAB (0.05%) for 10 min at room temperature. Images were analyzed to calculate the positive expression of phosphorylation of extracellular receptor kinase (ERK) and glycogen synthase kinase-3 β (GSK-3 β). Positive area <10% was graded as (-), positive area between 10-30% was graded as (+) while positive area >30% was graded as (++)

TEM. Following 6 h of reperfusion, electron microscopic analysis of liver tissue was performed to observe subcellular modification. Liver samples were first fixed in a 1% osmic acid fixative solution for 3 h at 4°C. Fixed samples were dehydrated with graded ethanol solution followed by ethanol/acetone solutions and 90% acetone. Following washing with PBS, dehydrated samples were embedded in acetone: OCT compound (2:1) for 4 h. Tissues were finally embedded in 100% embedding medium and dried (at 37°C overnight, 45°C for 12 h and 60°C for 24 h). Dried samples were sliced into 50-nm sections and observed under a transmission electron microscope (Crossbeam 550 FE; Carl Zeiss AG) following staining

with 2% uranyl acetate and lead citrate at room temperature for 10 min. Embedding medium and staining solutions were provided by Microscopy Core Facility of Westlake University.

Western blot analysis. Protein expression levels of ERK1/2, phosphorylated (p)-ERK1/2, GSK-3 β , p-GSK-3 β , Bcl-2 and Bax were evaluated using western blotting as per standard protocol. The liver lysate was obtained by homogenizing the liver tissue in RIPA lysis buffer (cat. no. P0013B; Beyotime Institute of Biotechnology) followed by centrifugation at 12,000 x g at 4°C for 15 min. A total of 40 μ g of protein sample, following quantification using a BCA kit, were separated using 10% SDS-PAGE and transferred to PVDF membranes. Non-specific binding of antibodies was blocked by incubation in 5% BSA for 32 h at 4°C. Blots were further incubated at 4°C overnight with respective primary antibodies: ERK1/2 (1:1,000; product no. 4695), p-ERK1/2 (1:2,000; product no. 4370), GSK-3 β (1:1,000; product no. 5676), p-GSK-3 β (1:1,000; product no. 9322; all from Cell Signaling Technology, Inc.), Bcl-2 mouse monoclonal antibody (1:1,000; 60178-1-Ig; ProteinTech Group, Inc.), Bax rabbit monoclonal antibody (1:1,000; cat. no. 60267-1-Ig; ProteinTech Group, Inc.) and GAPDH (1:1,000; product no. 5174; Cell Signaling Technology, Inc.) followed by incubation with goat anti-rabbit IgG HRP-linked secondary antibody (1:2,000; cat. no. 7074; Cell Signaling Technology, Inc.) for 1.5 h at 25°C. Blots were washed with TBS with 0.05% Tween-20 (TBST) thrice and a chemiluminescence reaction was achieved with an ECL reagent (cat. no. 34076; Thermo Fisher Scientific, Inc.) for visualization. Images were captured using an image analysis system (model GIS-1000; Tanon Science and Technology Co., Ltd.). Western blot images were further analyzed using ImageJ software (version 1.51j8; National Institutes of Health) to determine the relative expression of proteins.

Reverse transcription-quantitative (RT-q)PCR. In addition to immunohistochemistry and western blotting, RT-qPCR was also performed to analyze the expression of ERK1/2 and GSK-3 β . Total RNA was extracted using TRIzol LS and TRIzol (Invitrogen, Thermo Fisher Scientific, Inc.) according to the manufacturer's protocol. Subsequently, the concentration and purity of obtained RNA were determined by Nano-Drop spectrophotometer (Thermo Fisher Scientific, Inc.), and if the OD_{260/280} was in the range of ~1.8-2.0 this was deemed as acceptable. Then, the expression level of genes was examined by RT-qPCR with the SYBR Green I (Takara Bio, Inc.) dye detection method according to the manufacturer's protocol. The thermocycling conditions were as follows: Denaturation at 95°C for 5 min followed by annealing at 60°C for 15 sec and extension at 72°C for 25 sec (40 cycles). A total of 1 μ g of total RNA from each sample was reverse-transcribed using Takara reverse transcription kit (cat. no. 639505, Takara Bio, Inc.) following the manufacturer's protocol. β -actin was used as a loading control. The primers were as follows: β -actin forward, 5'-CCC GCGAGTACAACCTTCT-3' and reverse, 5'-CGTCAT CCATGGCGAACT-3'; ERK1/MAPK3 (248 bp) forward, 5'-TCCGCCATGAGAATGTTATAGGC-3' and reverse, 5'-GGTGGTGTGATAAGCAGATTGG-3'; ERK2/MAPK1 (84 bp) forward, 5'-GGTTGTTCCCAAATGCTGACT-3' and reverse, 5'-CAACTTCAATCCTCTTGTGAGGG-3'; and

GSK-3 β (200 bp) forward, 5'-TATGGTCTGCAGGCTGT GTG-3' and reverse, 5'-CCGAAAGACCTTCGTCCAA-3'. Finally, the cycle threshold (Cq) of each sample was detected using ABI 7900 thermocycler (Applied Biosystems; Thermo Fisher Scientific, Inc.), and the relative expression of genes was calculated using 2^{- $\Delta\Delta$ Cq} method (24). Each experiment was repeated three times.

Statistical analysis. All data were presented as the mean \pm standard deviation (SD) (n=6). Comparison between different groups was performed using one-way ANOVA followed by Tukey's post hoc test. Statistical analysis was performed using GraphPad Prism software, version 8.0.2 (GraphPad Software, Inc.). P<0.05 was considered to indicate a statistically significant difference.

Results

Identification of isolated ADSCs and ADSCs-exo. Isolated ADSCs were identified using surface markers. Fig. 2A reveals CD73, CD90 and CD105 on cell surfaces that are positive markers for ADSCs. Negative expression of CD34, CD45 and CD11b was also observed for ADSCs as revealed in Fig. 2B. Furthermore, isolated exosomes from ADSCs were also confirmed using surface markers such as TSG101, CD9 and CD63 through western blot analysis as revealed in Fig. 2C. The morphology and size of exosomes were evaluated by TEM, and the images obtained revealed spherical vesicular shape with a size range of 80-150 nm (Fig. 2D). Isolation of exosomes is a critical step and several methods have been reported. All methods have advantages and disadvantages; however, no consensus exists between researchers on a single method. Ultracentrifugation is a commonly employed method for isolation of exosomes and was used in the present study as it does not significantly affect the protein and RNA content of exosomes (25).

Effect on liver enzymes. Serum concentrations of AST, ALT and LDH were quantified for three groups as revealed in Fig. 3. The PBS + I/R rats exhibited higher concentrations of all markers indicating hepatic damage following 2 and 6 h of perfusion. In the case of exosome-treated rats, AST, ALT and LDH concentrations were higher than those of the sham group; however, their concentrations were significantly lower than the PBS + I/R group (Fig. 3). These results demonstrated that exosome treatment could prevent hepatocyte damage induced by hepatic I/R injury.

Ultrastructural modification of cellular components. TEM was performed to observe subcellular structures of hepatocytes following 6 h reperfusion. Hepatocytes in the sham group exhibited normal features of nuclei, mitochondria and endoplasmic reticulum (Fig. 4A). The PBS + I/R group exhibited typical structural changes of I/R injury including swelling of mitochondria with visible cristae, dilation of hepatic sinuses, swelling of the endoplasmic reticulum, presence of Kupffer cells and the nuclei of hepatocytes exhibited pyknosis (Fig. 4B). In the ADSCs-exo + I/R group, nuclei were slightly swollen, the endoplasmic reticulum was slightly widened, while no noticeable swelling was observed in mitochondria

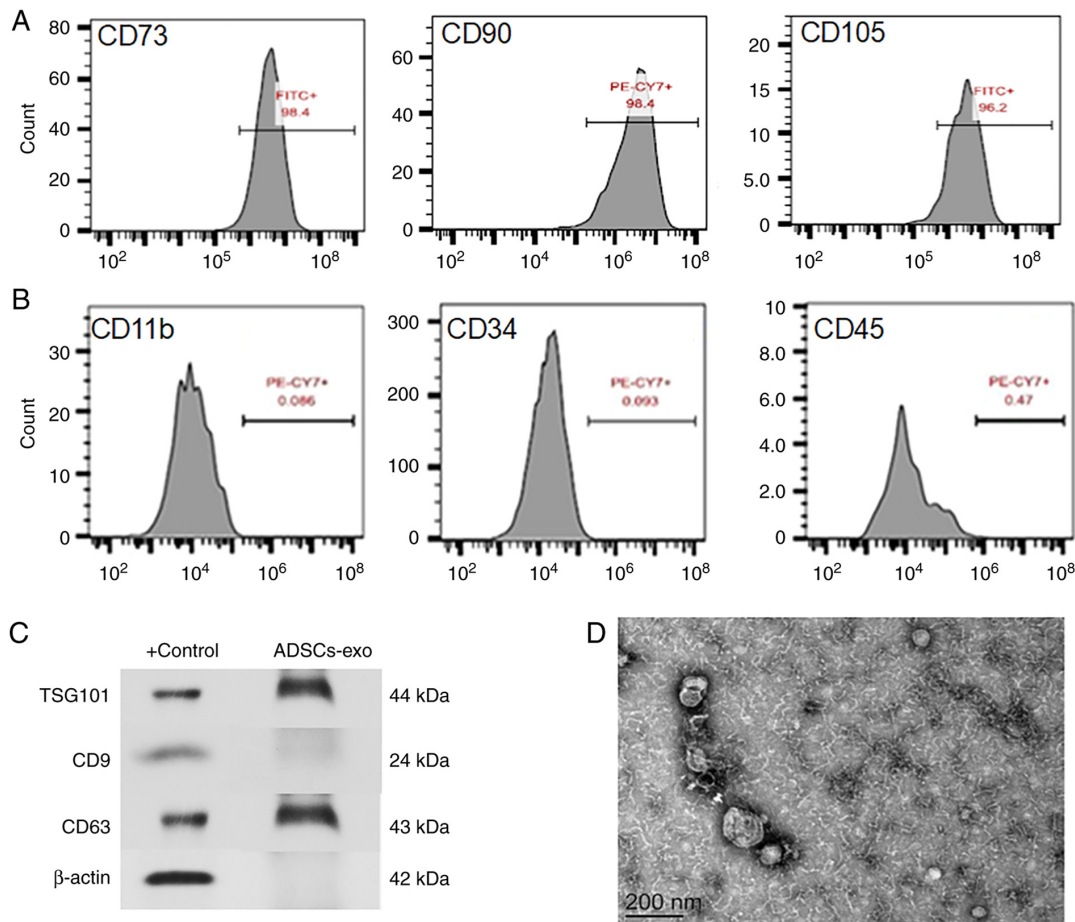


Figure 2. Identification of isolated ADSCs and ADSCs-exo. (A) Expression of surface positive markers CD73, CD90 and CD105 on ADSCs. (B) Expression of negative markers CD11b, CD34 and CD45 on ADSCs. (C) Expression of TSG101, CD9 and CD63 on ADSCs-exo. (D) Image of isolated exosomes obtained using transmission electron microscopy. ADSCs-exo, exosomes from adipose-derived stem cells.

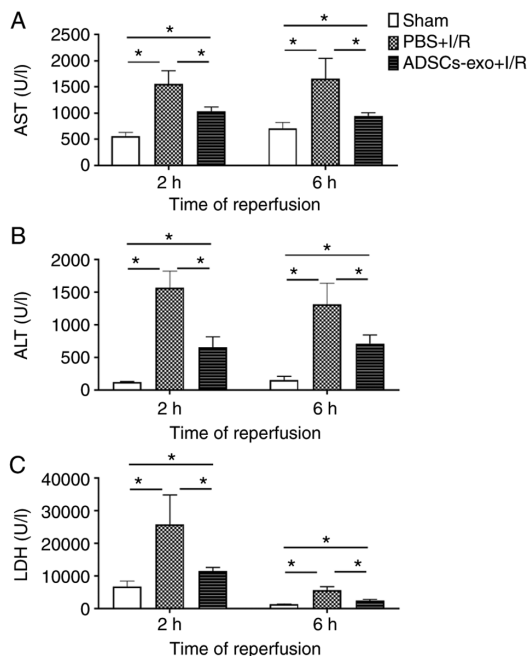


Figure 3. Serum biochemical markers (A) aspartate aminotransferase, (B) alanine aminotransferase and (C) lactate dehydrogenase of the sham group, the PBS + I/R group and the ADSCs-exo + I/R group (n=6). *P<0.005. AST, aspartate aminotransferase; ALT, alanine aminotransferase; LDH, lactate dehydrogenase; I/R, ischemia-reperfusion; ADSCs-exo, exosomes from adipose-derived stem cells.

(Fig. 4C). Collectively, ADSCs-exo treatment was found to attenuate the I/R injury effect on subcellular components.

Influence of ADSCs-exo on necrosis and apoptosis. The protective effect of ADSCs-exo against I/R injury was further evaluated using necrosis and apoptosis. H&E-stained images of liver samples of all groups following 2 and 6 h of reperfusion are presented in Fig. 5A. The sham group exhibited no significant liver tissue necrosis (Fig. 5A and B). The PBS + I/R group exhibited a significantly higher necrotic area which was evidence of I/R injury (Fig. 5B). In addition, with ADSCs-exo treatment, a significant reduction in the necrotic area was observed which indicated the efficacy of ADSCs-exo in protecting against I/R injury (Fig. 5A and B). Similarly, the PBS + I/R group exhibited a higher number of apoptotic cells as determined by TUNEL staining of liver sections following 2 and 6 h of reperfusion (Fig. 5C and D). ADSCs-exo pre-treatment produced a significant reduction in apoptotic cells as revealed in Fig. 5C and D. Collectively, it was demonstrated that ADSCs-exo pre-treatment produced a significant reduction in liver tissue necrosis and apoptosis caused by I/R injury.

Analysis of oxidative stress and lipid peroxidation due to I/R injury. For oxidative stress evaluation, the concentration of SOD and ROS activity in liver homogenates were quantified.

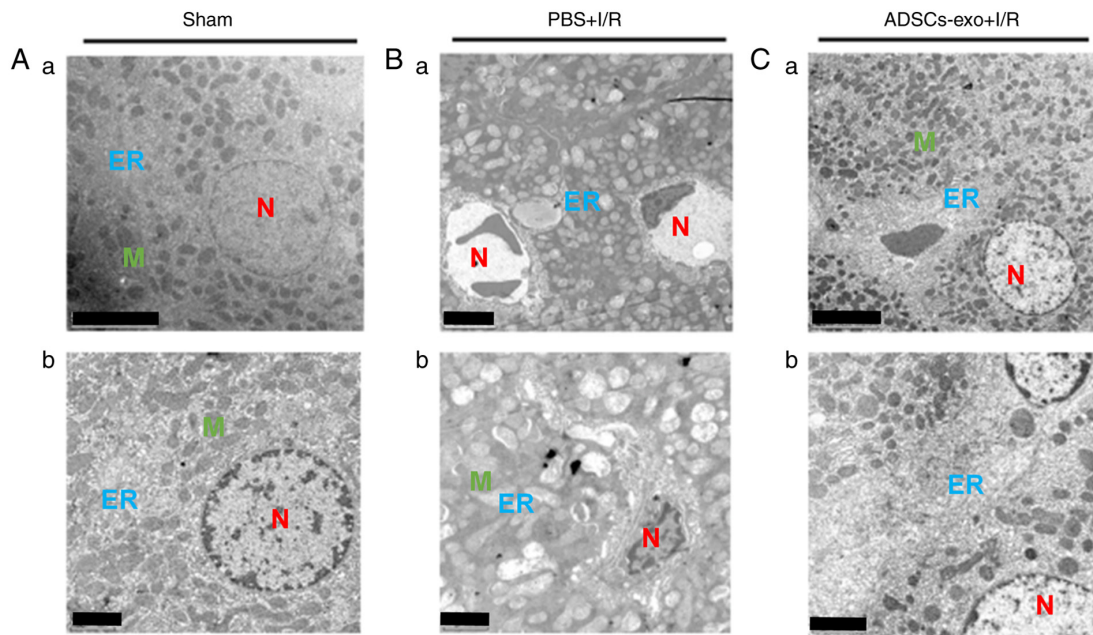


Figure 4. Ultrastructure morphological analysis of hepatocytes isolated from (A-a) sham rats following 6 h of reperfusion, (B-a) rats from the PBS + I/R group and (C-a) the ADSCs-exo + I/R group. (A-b, B-b and C-b) are the magnified images of A-a, B-a and C-a, respectively. Scale bar, 5 μm for A-a, B-a and C-a; 2 μm for A-b, B-b and C-b. ER, endoplasmic reticulum; N, nucleus; K, Kupffer cells; M, mitochondria; I/R, ischemia-reperfusion; ADSCs-exo, exosomes from adipose-derived stem cells.

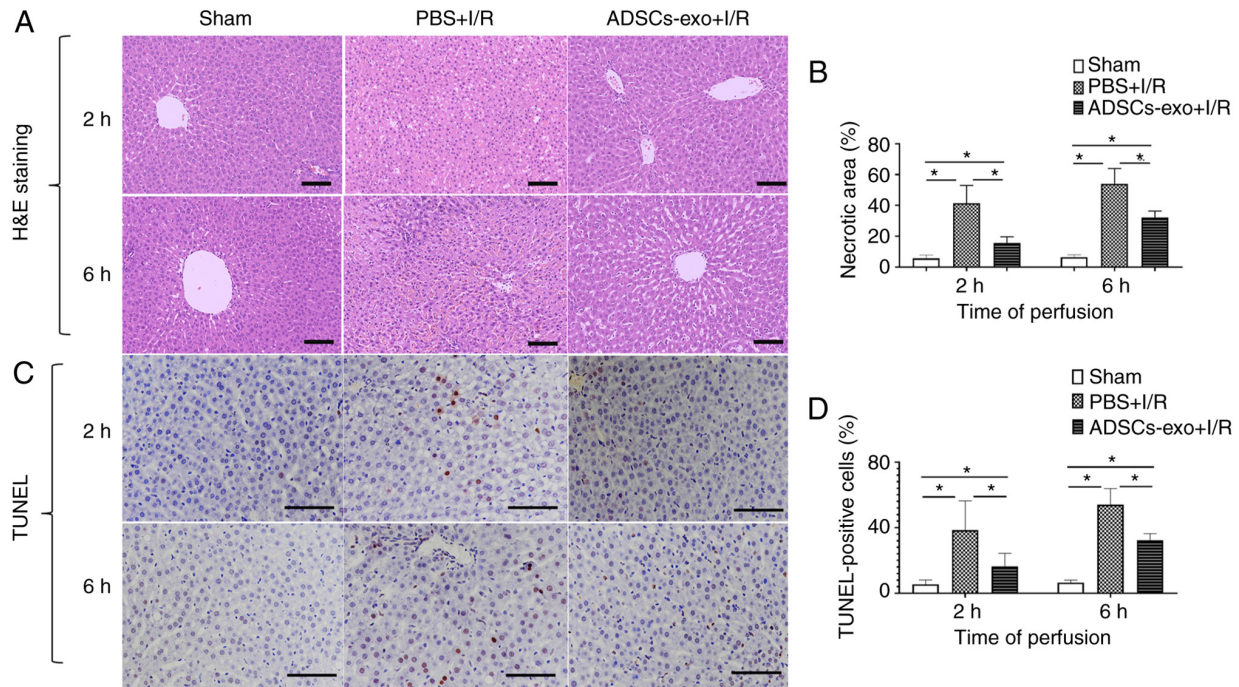


Figure 5. (A) Images from H&E staining of the liver revealing necrotic areas after 2 and 6 h of reperfusion. (B) Comparison of necrosis in different groups. (C) Images from TUNEL staining of the liver tissue after 2 and 6 h of reperfusion. (D) Comparison of apoptosis (TUNEL-positive cells) in different groups. Scale bar, 100 μm . * $P < 0.05$. I/R, ischemia-reperfusion; ADSCs-exo, exosomes from adipose-derived stem cells; TUNEL, TdT-mediated dUTP nick-end labeling.

A lower concentration level of SOD was observed in the PBS + I/R group following 2 and 6 h of reperfusion compared with the sham group (Fig. 6A). This reduced level of SOD also increased ROS in the PBS + I/R group (Fig. 6B). Regarding ADSCs-exo pre-treatment, a significant increase in SOD was revealed to reduce the oxidative stress by reducing ROS (Fig. 6A and B). Reduction in ROS may protect hepatocytes

from damage induced by I/R injury. Furthermore, MDA was also quantified as a marker for lipid peroxidation. Higher MDA was observed in the PBS + I/R group as compared with the ADSCs-exo-treated rats indicating that ADSCs-exo could reduce lipid peroxidation (Fig. 6C). In summary, ADSCs-exo treatment caused a reduction in oxidative stress and consequently a reduction in lipid peroxidation.

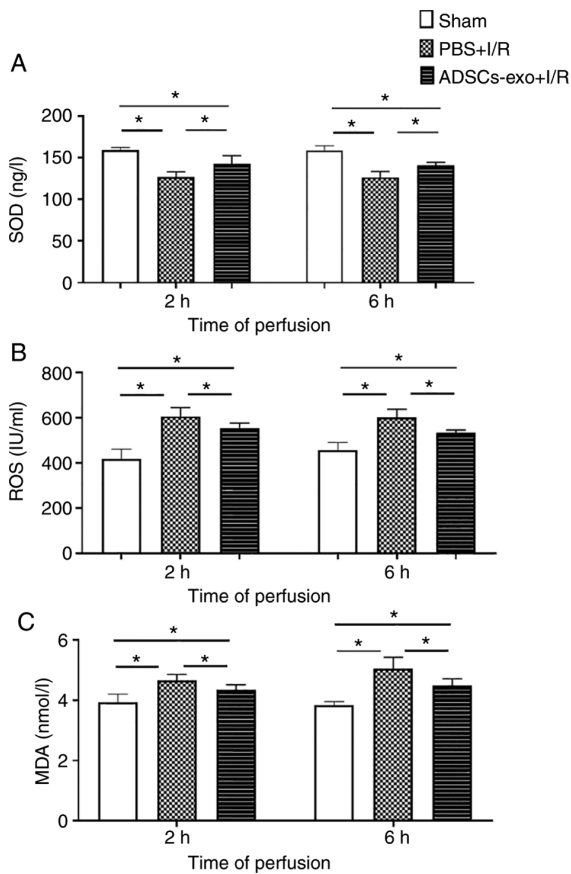


Figure 6. Quantification of (A) superoxide dismutase, (B) reactive oxygen species and (C) malondialdehyde in the liver of rats of the sham group, the PBS + I/R group and the ADSCs-exo group after 2 and 6 h of reperfusion (n=6). *P<0.05. SOD, superoxide dismutase; ROS, reactive oxygen species; MDA, malondialdehyde; I/R, ischemia-reperfusion; ADSCs-exo, exosomes from adipose-derived stem cells.

Inflammatory markers. IL-1 β and TNF- α (inflammatory cytokines) in serum are markers of neutrophil activation and reported to be increased in I/R injury (26). The PBS + I/R group exhibited a higher concentration of IL-1 β and TNF- α than the ADSC-exo-treated rats following 2 and 6 h of reperfusion as revealed in Fig. 7. The sham group showed lower values for inflammatory markers as compared with both the PBS + I/R and ADSCs-exo + I/R groups (Fig. 7). ADSCs-exo treatment could reduce inflammatory accumulation of inflammatory cytokines, thus, protecting the liver damage from such mediators.

Analysis of expression of ERK and GSK-3 β . ERK1/2 and GSK-3 β were evaluated using immunohistochemical analysis as these pathways have been reported to attenuate ischemic injury by reducing apoptosis and oxidative stress (27,28). As shown in Fig. 8A, phosphorylation of ERK1/2 and GSK-3 β were revealed to be increased in the ADSCs-exo-treated rats. Furthermore, p-ERK1/2 and p-GSK-3 β upregulation was also confirmed by western blot analysis following 2 h of reperfusion which revealed a higher ratio of p-ERK/ERK and p-GSK-3 β /GSK-3 β in the ADSCs-exo-treated rats compared with the PBS + I/R group (Fig. 8B and C). In the sham group lower expression of p-GSK-3 β was due to lack of I/R injury. ADSCs-exo caused phosphorylation of ERK1/2 and GSK-3 β in the liver contributing to a protective effect against damage.

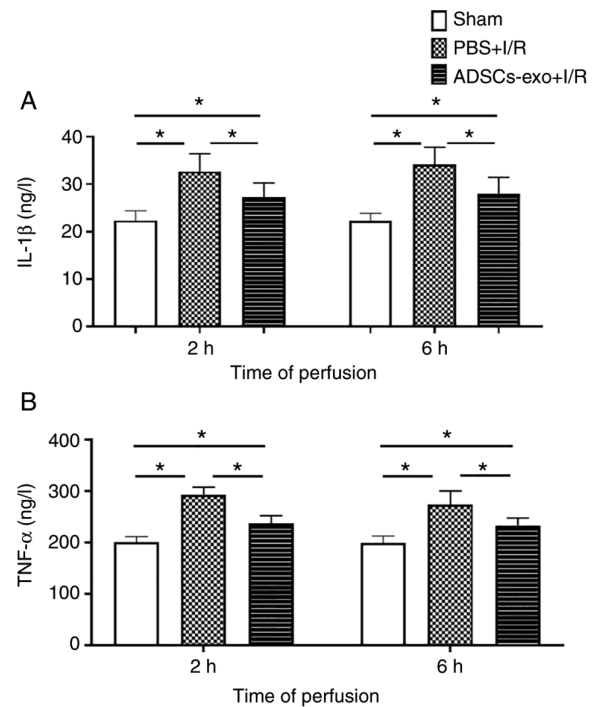


Figure 7. Quantification of inflammatory cytokines, (A) IL-1 β and (B) TNF- α in the serum of rats after 2 and 6 h of reperfusion (n=6). *P<0.05. I/R, ischemia-reperfusion; ADSCs-exo, exosomes from adipose-derived stem cells.

For further validation of results, RT-qPCR was also performed which revealed significantly higher expression levels of ERK1 and GSK-3 β in the ADSCs-exo-treated rats compared with the PBS + I/R group. However, no significant increase was observed in the expression of ERK2 (Fig. 9).

Bax and Bcl-2. Relative expression of Bax and Bcl-2 is important to determine apoptotic behavior. As revealed in Fig. 10A, higher Bcl-2 expression was observed in the ADSCs-exo-treated group compared with the PBS + I/R group.

PGE2 and cAMP levels. PGE2 levels in the sham, PBS + I/R and ADSCs-exo + I/R groups are presented in Fig. 10B, which revealed a significantly higher concentration of PGE2 in the ADSCs-exo + I/R group after 6 h of reperfusion compared to both the sham and PBS + I/R groups. Furthermore, a similar behavior was observed in the case of cAMP levels (Fig. 10C).

Discussion

ADSCs may easily be obtained through minimally invasive surgical procedures and have been explored in various therapeutic applications (29). However, several drawbacks exist concerning the application of stem cells as a therapeutic tool (13,14). Recently, ADSCs-exo or components of ADSCs-exo have exhibited protective potential against a number of health issues including peripheral nerve injury (30), erectile dysfunction (31,32), ischemic stroke (33), wound healing (34), stress urinary incontinence (35) and cardiomyocyte apoptosis caused by ischemia (36). Based on these studies, it was hypothesized that ADSCs-exo may potentially

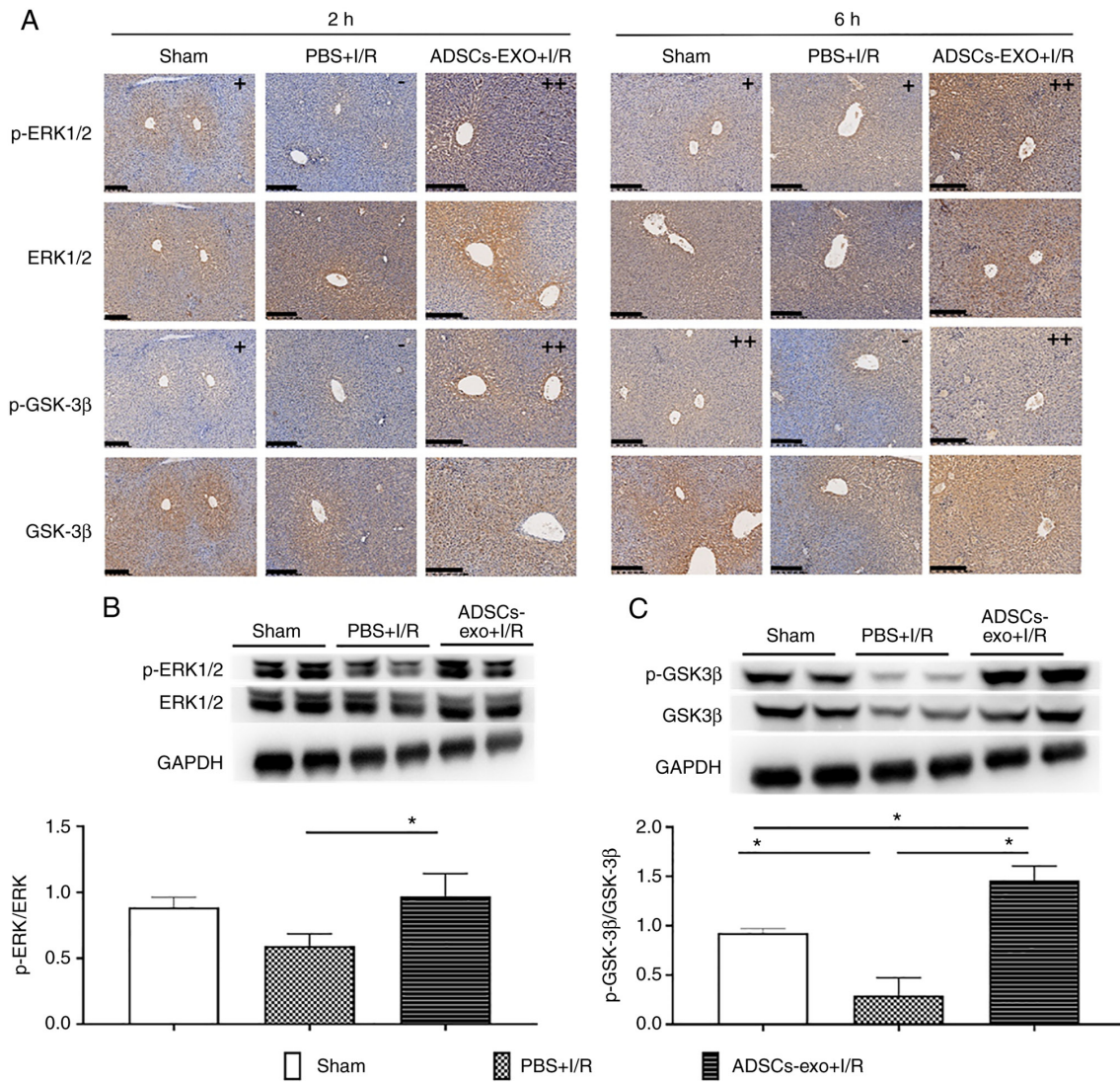


Figure 8. Expression of ERK1/2, p-ERK1/2, GSK-3 β and p-GSK-3 β . (A) Immunohistochemical staining of ERK1/2, p-ERK1/2, GSK-3 β and p-GSK-3 β after 2 and 6 h of reperfusion (scale bar, 200 μ m). Positive area <10% was graded as (-), positive area between 10-30% was graded as (+) while positive area >30% was graded as (++) Expression quantification of relative (B) p-ERK1/2 and (C) p-GSK-3 β using western blot analysis. * P <0.05. ERK, extracellular receptor kinase; p-, phosphorylated; GSK-3 β , glycogen synthase kinase-3 β ; I/R, ischemia-reperfusion; ADSCs-exo, exosomes from adipose-derived stem cells.

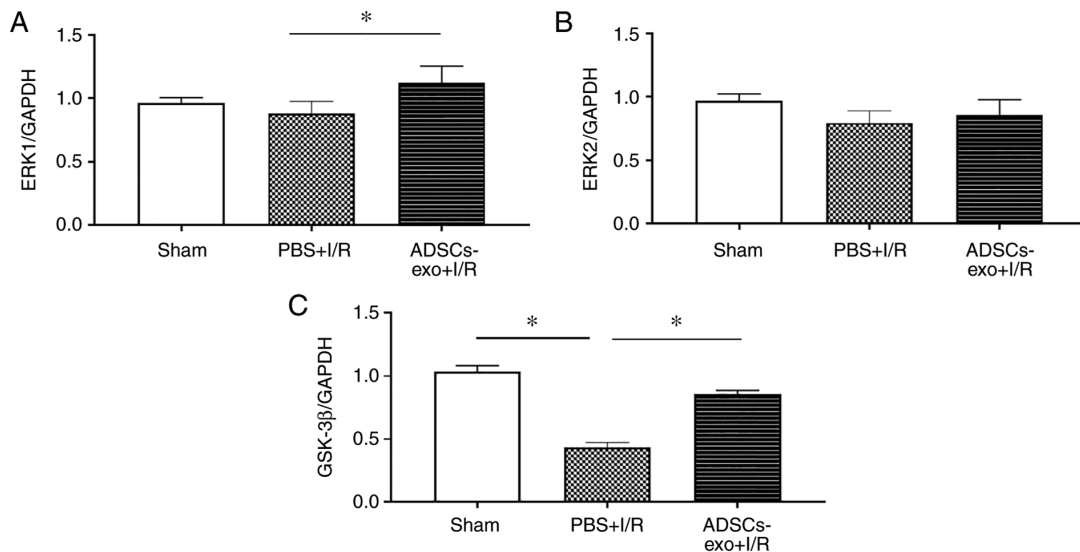


Figure 9. Relative expression of (A) ERK1, (B) ERK2 and (C) GSK-3 β quantified using reverse transcription-quantitative PCR. * P <0.05. ERK, extracellular receptor kinase; GSK-3 β , glycogen synthase kinase-3 β ; I/R, ischemia-reperfusion; ADSCs-exo, exosomes from adipose-derived stem cells.

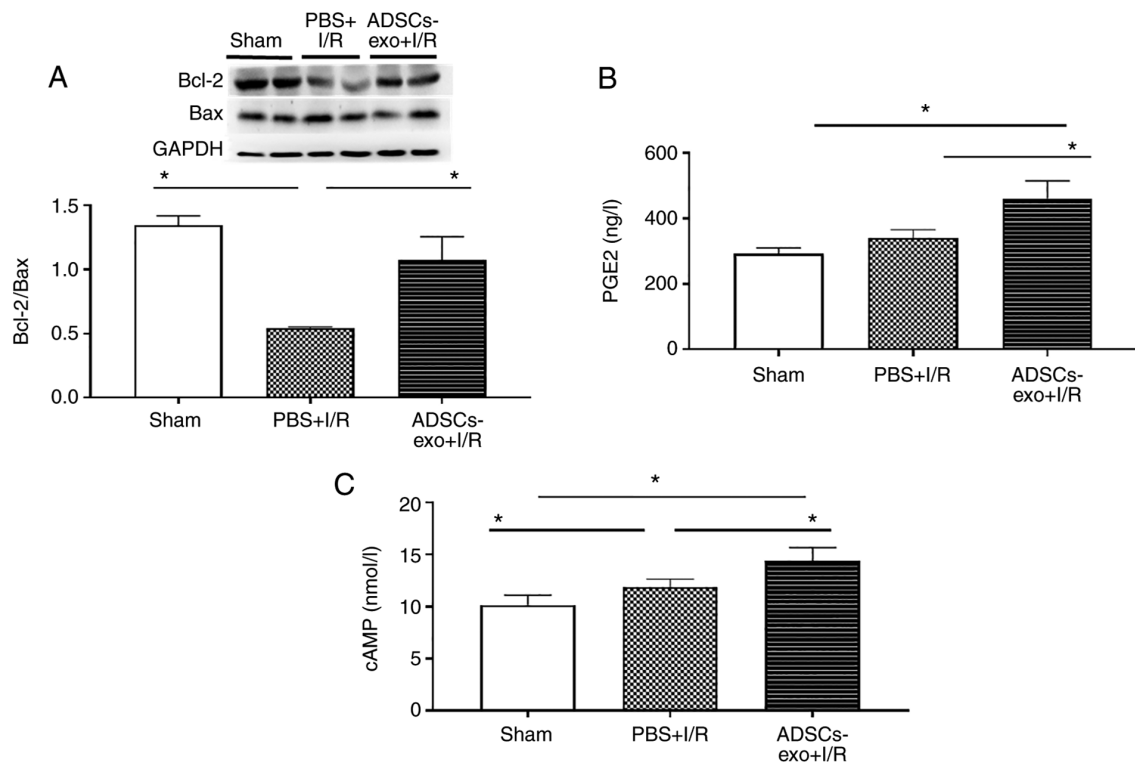


Figure 10. (A) Relative expression of Bcl-2/Bax in the liver from different groups quantified with respect to GAPDH expression after 6 h of reperfusion. (B) PGE2 concentration level after 6 h of reperfusion. (C) cAMP concentration level after 6 h of reperfusion. * $P < 0.05$. PGE2, prostaglandin E2; I/R, ischemia-reperfusion; ADSCs-exo, exosomes from adipose-derived stem cells.

protect hepatic I/R injury through reduction of apoptosis by countering oxidative stress caused by hypoxia.

The largest parenchymal organ in mammals is the liver which performs several important biological functions including metabolism of biomolecules (lipids, proteins and carbohydrates), secretion of bile to aid digestion and detoxification of endo/exogenous toxins (37). Hepatic I/R injury is a common cause of postoperative morbidity/mortality during hepatectomy, transplantation or trauma (38). Hypoxia and generation of ROS are considered major contributors to hepatic damage by I/R injury (39). ROS may cause DNA damage, lipid peroxidation and apoptosis of hepatocytes (40,41). Additionally, the release of inflammatory mediators further exacerbates apoptosis and tissue damage (42). In the present study, pre-treatment with ADSCs-exo revealed a reduction of ROS, an increase in SOD concentration and decreases in IL-1 β and TNF- α expression levels, thus reducing apoptosis/necrosis. Electron microscopy revealed stable subcellular structures of hepatocytes for ADSCs-exo-treated rats as compared with the PBS + I/R group. Furthermore, high expression of p-ERK and p-GSK-3 β was revealed with ADSCs-exo treatment.

GSK-3 β inactivation (phosphorylation) has been reported to protect organs against I/R injury as a self-regulatory mechanism (43,44). The inactivation of GSK-3 β may cause accumulation of β -catenin via the GSK-3 β / β -catenin signaling pathway, which has been revealed to increase anti-apoptotic protein expression (Bcl-2 and survivin) in cells (28). GSK-3 β was also revealed to be involved in inducing mitochondrial permeability transition pore (MPTP) that leads to mitochondria-mediated cell death (45,46). Phosphorylation (inactivation) of GSK-3 β inhibited the induction of MPTP via

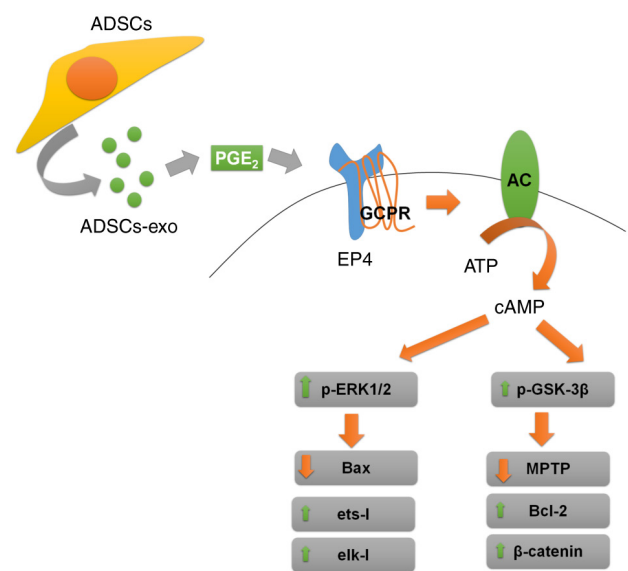


Figure 11. Schematic diagram of the proposed mechanistic processes involved in the hepatoprotective activity of ADSCs-exo. ADSCs-exo, exosomes from adipose-derived stem cells; EP4, prostaglandin E receptor subtype; ERK, extracellular receptor kinase; GSK-3 β , glycogen synthase kinase-3 β .

ANT interaction which is also considered a protective effect of inactivation of GSK-3 β against I/R injury. In the present study, an increase in Bcl-2 was revealed following 6 h of reperfusion due to overexpression of p-GSK-3 β .

In addition to GSK-3 β inactivation, ADSCs-exo treatment was also found to upregulate ERK1/2 which was also a contributor to the protective effect of exosomes against I/R

injury. Activation (phosphorylation) of ERK was reported to occur in I/R injury of different organs including the liver. This upregulation of ERK1/2 with ADSCs-exo treatment was revealed to be consistent with a recent study (47). ERKs are considered to induce an anti-apoptotic effect via reduction of Bax protein and an increase of Bcl-2 (48). Recently, Cai *et al* reported a prostaglandin E receptor subtype (EP4)-mediated hepatoprotective effect against I/R injury in rat model via ERK1/2 activation (49). In another recent study, Gao *et al* used a limb ischemic post-conditioning technique to counteract hepatic I/R injury (50). They identified activation of ERK1/2 as a key mechanism in the prevention of hepatic I/R injury. In addition, ERK1/2 activation-mediated cell survival was also reported by overexpression of Ets-I and Elk-I transcription factors, which promoted cell growth and proliferation (51,52). In the present study, an increase in the expression of ERK1/2 was revealed as an ADSCs-exo-mediated protective mechanism. The downregulation of Bax mediated by ERK1/2 following 6 h of reperfusion in the ADSCs-exo-treated rats as compared with the PBS + I/R group, produced fewer apoptotic cells.

In our previous study, EP4 activation was revealed to ameliorate hepatic I/R injury via ERK1/2 and GSK-3 β -mediated MPTP inhibition (49). Stem cell-derived exosomes were reported to carry PGE2 which is a ligand of EP4 (53,54). From this perspective, it is proposed that activation of ERK1/2 and inactivation GSK-3 β mediated by ADSCs-exo was due to PGE2 via secondary messenger-cAMP. In the present study, higher PGE2 and cAMP levels were also found in ADSCs-exo-treated rats compared with the PBS + I/R group, which validated the PGE2-mediated protective effect of ADSCs-exo. A schematic diagram of the mechanism involved in the protective effect of exosomes against hepatic I/R injury is presented in Fig. 11. There may be other components of exosomes such as heat shock protein-70 (HSP70) which could also be responsible for the protective effect of exosomes against hepatic I/R injury (55). In addition, another component of exosomes that may play an important role in the protection from I/R injury is miR-126 which was reported to be effective against acute myocardial infarction (56). However, the present study proposed PGE2 as an important factor in I/R injury. Further study may be conducted to evaluate the hepatoprotective effect of these other components. ADSCs-exo were established as a potential therapeutic tool in the protection against hepatic I/R; however, general limitations such as lack of homogeneity, batch-to-batch variation and quality control for isolated exosomes still need to be addressed.

In conclusion, the present study revealed the potential of ADSCs-exo in ameliorating hepatic I/R injury in a rat model. ERK1/2 activation and GSK-3 β inactivation was observed via an increase in G-protein receptor-mediated cAMP, and these signaling pathways were found to reduce the effects of I/R injury. The present study was based on single dose model via portal vein administration. Further study for detailed exploration of the protective mechanism of ADSCs-exo with different administration routes and dosages should be considered in future research.

Acknowledgements

Not applicable.

Funding

The present study was supported by the National Natural Science Foundation of China (grant nos. 81670564 and 81470847) and the Youth Project of the National Natural Science Foundation of China (grant no. 81800554).

Availability of data and materials

The datasets used or analyzed during the current study are available from the corresponding author on reasonable request.

Authors' contributions

YZ, YL and QW performed the experiments, analyzed the data and drafted the manuscript. DZ, XF, WZ, LC and QZ helped to conduct the experiments and analysis. HF and HX conceived and designed the study and edited the final manuscript. YZ and QW confirmed the authenticity of raw data. All authors read and approved the final version of the manuscript.

Ethical approval and consent to participate

All procedures in the present study were conducted in accordance with the Guide for the Care and Use of Laboratory Animals of the National Institutes of Health and was approved (approval no. 00100097) by the Medical Ethics Committee of Naval Medical University (Shanghai, China).

Patient consent for publication

Not applicable.

Competing interests

The authors declare that they have no competing interests.

References

1. Cannistrà M, Ruggiero M, Zullo A, Gallelli G, Serafini S, Maria M, Naso A, Grande R, Serra R and Nardo B: Hepatic ischemia reperfusion injury: A systematic review of literature and the role of current drugs and biomarkers. *Int J Surg* 33 (Suppl 1): S57-S70, 2016.
2. Rampes S and Ma D: Hepatic ischemia-reperfusion injury in liver transplant setting: Mechanisms and protective strategies. *J Biomed Res* 33: 221-234, 2019.
3. Ding W, Duan Y, Qu Z, Feng J, Zhang R, Li X, Sun D, Zhang X and Lu Y: Acidic microenvironment aggravates the severity of hepatic ischemia/reperfusion injury by modulating M1-polarization through regulating PPAR- γ signal. *Front Immunol* 12: 697362, 2021.
4. Granger DN and Kvietys PR: Reperfusion injury and reactive oxygen species: The evolution of a concept. *Redox Biol* 6: 524-551, 2015.
5. van Golen RF, Reiniers MJ, Marsman G, Alles LK, van Rooyen DM, Petri B, Van der Mark VA, van Beek AA, Meijer B, Maas MA, *et al*: The damage-associated molecular pattern HMGB1 is released early after clinical hepatic ischemia/reperfusion. *Biochim Biophys Acta Mol Basis Dis* 1865: 1192-1200, 2019.
6. Go KL, Lee S, Zendejas I, Behrns KE and Kim JS: Mitochondrial dysfunction and autophagy in hepatic ischemia/reperfusion injury. *Biomed Res Int* 2015: 183469, 2015.

7. Zhang H, Yan Q, Wang X, Chen X, Chen Y, Du J and Chen L: The role of mitochondria in liver ischemia-reperfusion injury: From aspects of mitochondrial oxidative stress, mitochondrial fission, mitochondrial membrane permeable transport pore formation, mitophagy, and mitochondria-related protective measures. *Oxid Med Cell Longev* 2021: 6670579, 2021.
8. Chen Z, Ding T and Ma CG: Dexmedetomidine (DEX) protects against hepatic ischemia/reperfusion (I/R) injury by suppressing inflammation and oxidative stress in NLRC5 deficient mice. *Biochem Biophys Res Commun* 493: 1143-1150, 2017.
9. Wang W, Wu L, Li J, Ji J, Chen K, Yu Q, Li S, Feng J, Liu T, Zhang J, *et al*: Alleviation of hepatic ischemia reperfusion injury by oleonic acid pretreating via reducing HMGB1 release and inhibiting apoptosis and autophagy. *Mediators Inflamm* 2019: 3240713, 2019.
10. Yu Q, Wu L, Liu T, Li S, Feng J, Mao Y, Fan X, Guo C and Wu J: Protective effects of levo-tetrahydropalmatine on hepatic ischemia/reperfusion injury are mediated by inhibition of the ERK/NF- κ B pathway. *Int Immunopharmacol* 70: 435-445, 2019.
11. Shi Y, Qiu X, Dai M, Zhang X and Jin G: Hyperoside attenuates hepatic ischemia-reperfusion injury by suppressing oxidative stress and inhibiting apoptosis in rats. *Transplant Proc* 51: 2051-2059, 2019.
12. Manne NDPK, Arvapalli R, Graffeo VA, Bandarupalli VVK, Shokuhfar T, Patel S, Rice KM, Gijupalli GK and Blough ER: Prophylactic treatment with cerium oxide nanoparticles attenuate hepatic ischemia reperfusion injury in sprague dawley rats. *Cell Physiol Biochem* 42: 1837-1846, 2017.
13. Zhang Y, Han F, Gu L, Ji P, Yang X, Liu M, Tao K and Hu D: Adipose mesenchymal stem cell exosomes promote wound healing through accelerated keratinocyte migration and proliferation by activating the AKT/HIF-1 α axis. *J Mol Histol* 51: 375-383, 2020.
14. Bai Y, Han YD, Yan XL, Ren J, Zeng Q, Li XD, Pei XT and Han Y: Adipose mesenchymal stem cell-derived exosomes stimulated by hydrogen peroxide enhanced skin flap recovery in ischemia-reperfusion injury. *Biochem Biophys Res Commun* 500: 310-317, 2018.
15. Saidi RF, Rajeshkumar B, Sharifabrizi A, Bogdanov AA, Zheng S, Dresser K and Walter O: Human adipose-derived mesenchymal stem cells attenuate liver ischemia-reperfusion injury and promote liver regeneration. *Surgery* 156: 1225-1231, 2014.
16. Saat TC, van den Engel S, Bijman-Lachger W, Korevaar SS, Hoogduijn MJ, IJzermans JN and de Bruin RW: Fate and effect of intravenously infused mesenchymal stem cells in a mouse model of hepatic ischemia reperfusion injury and resection. *Stem Cells Int* 2016: 5761487, 2016.
17. G Kugeratski F and Kalluri R: Exosomes as mediators of immune regulation and immunotherapy in cancer. *FEBS J* 288: 10-35, 2021.
18. Zhang ZG, Buller B and Chopp M: Exosomes-beyond stem cells for restorative therapy in stroke and neurological injury. *Nat Rev Neurol* 15: 193-203, 2019.
19. Gatti S, Bruno S, Deregibus MC, Sordi A, Cantaluppi V, Tetta C and Camussi G: Microvesicles derived from human adult mesenchymal stem cells protect against ischaemia-reperfusion-induced acute and chronic kidney injury. *Nephrol Dial Transplant* 26: 1474-1483, 2011.
20. Wang J, Mi Y, Wu S, You X, Huang Y, Zhu J and Zhu L: Exosomes from adipose-derived stem cells protect against high glucose-induced erectile dysfunction by delivery of corin in a streptozotocin-induced diabetic rat model. *Regen Ther* 14: 227-233, 2020.
21. Sengupta V, Sengupta S, Lazo A, Woods P, Nolan A and Bremer N: Exosomes derived from bone marrow mesenchymal stem cells as treatment for severe COVID-19. *Stem Cells Dev* 29: 747-754, 2020.
22. Ge Y, Zhang Q, Jiao Z, Li H, Bai G and Wang H: Adipose-derived stem cells reduce liver oxidative stress and autophagy induced by ischemia-reperfusion and hepatectomy injury in swine. *Life Sci* 214: 62-69, 2018.
23. Zeller R: Fixation, embedding, and sectioning of tissues, embryos, and single cells. *Curr Protoc Mol Biol* 7: 14.1.1-14.1.8, 1989.
24. Livak KJ and Schmittgen TD: Analysis of relative gene expression data using real-time quantitative PCR and the 2(-Delta Delta C(T)) method. *Methods* 25: 402-408, 2001.
25. Yu LL, Zhu J, Liu JX, Jiang F, Ni WK, Qu LS, Ni RZ, Lu CH and Xiao MB: A comparison of traditional and novel methods for the separation of exosomes from human samples. *Biomed Res Int* 2018: 3634563, 2018.
26. Konishi T and Lentsch AB: Hepatic ischemia/reperfusion: Mechanisms of tissue injury, repair, and regeneration. *Gene Expr* 17: 277-287, 2017.
27. Choi DE, Jeong JY, Choi H, Chang YK, Ahn MS, Ham YR, Na KR and Lee KW: ERK phosphorylation plays an important role in the protection afforded by hypothermia against renal ischemia-reperfusion injury. *Surgery* 161: 444-452, 2017.
28. Yan Y, Li G, Tian X, Ye Y, Gao Z, Yao J, Zhang F and Wang S: Ischemic preconditioning increases GSK-3 β / β -catenin levels and ameliorates liver ischemia/reperfusion injury in rats. *Int J Mol Med* 35: 1625-1632, 2015.
29. Huang T, He D, Kleiner G and Kuluz J: Neuron-like differentiation of adipose-derived stem cells from infant piglets in vitro. *J Spinal Cord Med* 30 (Suppl 1): S35-S40, 2007.
30. Liu CY, Yin G, Sun YD, Lin YF, Xie Z, English AW, Li QF and Lin HD: Effect of exosomes from adipose-derived stem cells on the apoptosis of Schwann cells in peripheral nerve injury. *CNS Neurosci Ther* 26: 189-196, 2020.
31. Zhu LL, Huang X, Yu W, Chen H, Chen Y and Dai YT: Transplantation of adipose tissue-derived stem cell-derived exosomes ameliorates erectile function in diabetic rats. *Andrologia* 50: e12871, 2018.
32. Chen F, Zhang H, Wang Z, Ding W, Zeng Q, Liu W, Huang C, He S and Wei A: Adipose-derived stem cell-derived exosomes ameliorate erectile dysfunction in a rat model of type 2 diabetes. *J Sex Med* 14: 1084-1094, 2017.
33. Jiang M, Wang H, Jin M, Yang X, Ji H, Jiang Y, Zhang H, Wu F, Wu G, Lai X, *et al*: Exosomes from miR-30d-5p-ADSCs reverse acute ischemic stroke-induced, autophagy-mediated brain injury by promoting M2 microglial/macrophage polarization. *Cell Physiol Biochem* 47: 864-878, 2018.
34. Li X, Xie X, Lian W, Shi R, Han S, Zhang H, Lu L and Li M: Exosomes from adipose-derived stem cells overexpressing Nrf2 accelerate cutaneous wound healing by promoting vascularization in a diabetic foot ulcer rat model. *Exp Mol Med* 50: 1-14, 2018.
35. Ni J, Li H, Zhou Y, Gu B, Xu Y, Fu Q, Peng X, Cao N, Fu Q, Jin M, *et al*: Therapeutic potential of human adipose-derived stem cell exosomes in stress urinary incontinence-an in vitro and in vivo study. *Cell Physiol Biochem* 48: 1710-1722, 2018.
36. Liu L, Zhang H, Mao H, Li X and Hu Y: Exosomal miR-320d derived from adipose tissue-derived MSCs inhibits apoptosis in cardiomyocytes with atrial fibrillation (AF). *Artif Cells Nanomed Biotechnol* 47: 3976-3984, 2019.
37. Dolganiuc A: Role of lipid rafts in liver health and disease. *World J Gastroenterol* 17: 2520-2535, 2011.
38. Cai L, Li Y, Zhang Q, Sun H, Yan X, Hua T, Zhu Q, Xu H and Fu H: Salidroside protects rat liver against ischemia/reperfusion injury by regulating the GSK-3 β /Nrf2-dependent antioxidant response and mitochondrial permeability transition. *Eur J Pharmacol* 806: 32-42, 2017.
39. Chen R, Lai UH, Zhu L, Singh A, Ahmed M and Forsyth NR: Reactive oxygen species formation in the brain at different oxygen levels: The role of hypoxia inducible factors. *Front Cell Dev Biol* 6: 132, 2018.
40. Srinivas US, Tan BWQ, Vellayappan BA and Jeyasekharan AD: ROS and the DNA damage response in cancer. *Redox Biol* 25: 101084, 2019.
41. Su LJ, Zhang JH, Gomez H, Murugan R, Hong X, Xu D, Jiang F and Peng ZY: Reactive oxygen species-induced lipid peroxidation in apoptosis, autophagy, and ferroptosis. *Oxid Med Cell Longev* 2019: 5080843, 2019.
42. Soares ROS, Losada DM, Jordani MC, Évora P and Castro-E-Silva O: Ischemia/reperfusion injury revisited: An overview of the latest pharmacological strategies. *Int J Mol Sci* 20: 5034, 2019.
43. Wang Y, Ge C, Chen J, Tang K and Liu J: GSK-3 β inhibition confers cardioprotection associated with the restoration of mitochondrial function and suppression of endoplasmic reticulum stress in sevoflurane preconditioned rats following ischemia/reperfusion injury. *Perfusion* 33: 679-686, 2018.
44. Xia Y, Rao J, Yao A, Zhang F, Li G, Wang X and Lu L: Lithium exacerbates hepatic ischemia/reperfusion injury by inhibiting GSK-3 β /NF- κ B-mediated protective signaling in mice. *Eur J Pharmacol* 697: 117-125, 2012.
45. Zhu J, Rebecchi MJ, Glass PS, Brink PR and Liu L: Cardioprotection of the aged rat heart by GSK-3 β inhibitor is attenuated: Age-related changes in mitochondrial permeability transition pore modulation. *Am J Physiol Heart Circ Physiol* 300: H922-H930, 2011.

46. Tanaka T, Saotome M, Katoh H, Satoh T, Hasan P, Ohtani H, Satoh H, Hayashi H and Maekawa Y: Glycogen synthase kinase-3 β opens mitochondrial permeability transition pore through mitochondrial hexokinase II dissociation. *J Physiol Sci* 68: 865-871, 2018.
47. An Y, Zhao J, Nie F, Qin Z, Xue H, Wang G and Li D: Exosomes from adipose-derived stem cells (ADSCs) overexpressing miR-21 promote vascularization of endothelial cells. *Sci Rep* 9: 12861, 2019.
48. Wang M, Lu X, Dong X, Hao F, Liu Z, Ni G and Chen D: pERK1/2 silencing sensitizes pancreatic cancer BXPC-3 cell to gemcitabine-induced apoptosis via regulating Bax and Bcl-2 expression. *World J Surg Oncol* 13: 66, 2015.
49. Cai LL, Xu HT, Wang QL, Zhang YQ, Chen W, Zheng DY, Liu F, Yuan HB, Li YH and Fu HL: EP4 activation ameliorates liver ischemia/reperfusion injury via ERK1/2-GSK3 β -dependent MPTP inhibition. *Int J Mol Med* 45: 1825-1837, 2020.
50. Gao Y, Zhou S, Wang F, Zhou Y, Sheng S, Qi D, Huang JH, Wu E, Lv Y and Huo X: Hepatoprotective effects of limb ischemic post-conditioning in hepatic ischemic rat model and liver cancer patients via PI3K/ERK pathways. *Int J Biol Sci* 14: 2037-2050, 2018.
51. Li Q, Eppolito C, Odunsi K and Shrikant PA: Antigen-induced Erk1/2 activation regulates Ets-1-mediated sensitization of CD8⁺ T cells for IL-12 responses. *J Leukoc Biol* 87: 257-263, 2010.
52. Godeny MD and Sayeski PP: ERK1/2 regulates ANGII-dependent cell proliferation via cytoplasmic activation of RSK2 and nuclear activation of elk1. *Am J Physiol Cell Physiol* 291: C1308-C1317, 2006.
53. Cosenza S, Ruiz M, Toupet K, Jorgensen C and Noël D: Mesenchymal stem cells derived exosomes and microparticles protect cartilage and bone from degradation in osteoarthritis. *Sci Rep* 7: 16214, 2017.
54. Liu J, Kuwabara A, Kamio Y, Hu S, Park J, Hashimoto T and Lee JW: Human mesenchymal stem cell-derived microvesicles prevent the rupture of intracranial aneurysm in part by suppression of mast cell activation via a PGE2-dependent mechanism. *Stem Cells* 34: 2943-2955, 2016.
55. Wu HH, Huang CC, Chang CP, Lin MT, Niu KC and Tian YF: Heat shock protein 70 (HSP70) reduces hepatic inflammatory and oxidative damage in a rat model of liver ischemia/reperfusion injury with hyperbaric oxygen preconditioning. *Med Sci Monit* 24: 8096-8104, 2018.
56. Luo Q, Guo D, Liu G, Chen G, Hang M and Jin M: Exosomes from MiR-126-overexpressing adscs are therapeutic in relieving acute myocardial ischaemic injury. *Cell Physiol Biochem* 44: 2105-2116, 2017.



This work is licensed under a Creative Commons Attribution-NonCommercial-NoDerivatives 4.0 International (CC BY-NC-ND 4.0) License.